J. Membrane Biol. 165, 275–282 (1998)

The Journal of
Membrane
Biology

Na^+-Coupled Alanine Transport in LLC-PK_1 Cells: The Relationship Between the K_m for Na^+ at Low [Alanine] and Potential Dependence for the System

J.J. Wilson*, J. Randles, G.A. Kimmich
Department of Biochemistry and Biophysics, School of Medicine and Dentistry, University of Rochester, Rochester, NY 14642, USA

Received: 10 April 1998/Revised: 6 July 1998

Abstract. Analysis of the mechanistic basis by which sodium-coupled transport systems respond to changes in membrane potential is inherently complex. Algebraic expressions for the primary kinetic parameters (K_m and V_{max}) consist of multiple terms that encompass most rate constants in the transport cycle. Even for a relatively simple cotransport system such as the Na^+/alanine cotransporter in LLC-PK_1 cells (1:1 Na^+ to substrate coupling, and an ordered binding sequence), the algebraic expressions for K_m for either substrate includes ten of the twelve rate constants necessary for modeling the full transport cycle. We show here that the expression of K_m of the first-bound substrate (Na^+) simplifies markedly if the second-bound substrate (alanine) is held at a low concentration so that its' binding becomes the rate limiting step. Under these conditions, the expression for the K_m^{Na} includes rate constants for only two steps in the full cycle: (i) binding/dissociation of Na^+, and (ii) conformational 'translocation' of the substrate-free protein. The influence of imposed changes in membrane potential on the apparent K_m^{Na} for the LLC-PK_1 alanine cotransporter at low alanine thus provides insight to potential dependence at these sites. The data show no potential dependence for K_m^{Na} at 5 μM alanine, despite marked potential dependence at 2 mM alanine when the full algebraic expression applies. The results suggest that neither translocation of the substrate-free form of the transporter nor binding/dissociation of extracellular sodium are potential dependent events for this transport system.

Key words: ASC transport system — Alanine transport — Sodium-coupled transport — Amino acid transport — Transport kinetics

Correspondence to: G.A. Kimmich

* *Present address:* Department of Pharmacology, Vanderbilt University, Nashville, TN 37232-6600, USA

Introduction

Sodium-coupled transport systems are biological 'machines' that harness energy released by flow of sodium ions down the electrochemical Na^+ gradient ($\Delta\mu_{na}$) that cells maintain across their plasma membrane to 'drive' the transfer of other ions or organic solutes against electrochemical gradients. Changes in membrane potential ($\Delta\Psi$) alter the free energy change for Na^+ flow via these transport systems, and can be expected to change flux of the cotransported substrate for those systems which catalyze a net charge transfer. Indeed, many sodium-coupled transport systems are responsive to changes in membrane potential [e.g. 2, 4, 7, 12, 21]. However, the molecular mechanism(s) responsible for potential-induced changes are not well understood.

Two conceptual ideas for potential dependence of Na^+-coupled systems have received particular attention. Transport models based on these concepts are sometimes categorized as either ''translocation'' or ''sodium-well' models. Translocation models propose that changes in membrane potential induce a conformational change in the transport protein that changes the side of the membrane from which substrates can gain access to their binding sites on the protein. These models have some features analogous to current models for voltage-gated ion channels where a potential driven conformational change in the channel protein alters the side of access for ions transferred through the channel [1, 8].

In contrast, sodium-well models assign potential dependence to events relating to binding or dissociation of Na^+ ions to/from the transport protein. These models propose sodium binding sites on the transport protein that are partially 'embedded' in the membrane matrix and thus are within the electric field represented by the membrane potential. Access channels with restricted selectivity admit sodium ions which 'feel' the influence of

the potential in reaching or leaving those sites. Changes in potential therefore influence the rate of Na^+ binding and/or dissociation from the protein. These models have features somewhat analogous to the ''proton-well'' model proposed by Mitchell [20] and Maloney [18] for describing the mechanism by which flow of H^+ down a gradient of electrochemical potential provides energy for the chemiosmotic coupling events that occur during oxidative phosphorylation. Because chemical affinity is defined as the ratio of rate constants governing ligand binding/dissociation events, these models predict potential-dependent changes in affinity of the transport protein for sodium.

Several investigators have attempted to analyze various sodium-coupled cotransport systems in hopes of determining which concept, translocation or sodium-well, best explains the basis for potential dependence in these systems [2–6, 9, 10, 12, 13, 16, 17, 21, 22]. Unfortunately, specific answers have been difficult to elucidate. With current experimental techniques, it is difficult to define conditions that allow accurate measurement of values for rate constants governing individual steps in the transport cycle. Instead, it is usually necessary to determine various ''kinetic'' parameters such as the Michaelis constant (K_m) or maximal velocity (V_{max}). Although K_m for a given solute is often interpreted as a surrogate for solute 'affinity' of the transport protein, this is an oversimplification. It is important to remember that even for the simplest cotransport systems, K_m and V_{max} are complex algebraic expressions that include rate constants for most steps in the transport cycle. Therefore, potential dependence for either parameter does not necessarily provide any insight to specific sites in the transport cycle that are responsive to changes in membrane potential.

This report describes work relating to a particular set of experimental conditions in which the usual complex expression for the K_m^{Na} for the Na^+/alanine cotransporter simplifies to one which has rate constants for only two steps in the full transport cycle. Data obtained at different membrane potentials under these conditions were analyzed to determine whether either of these two loci exhibit potential dependence.

Materials and Methods

Cell Culture

Frozen stocks of LLC-PK_1 cells, at passage 196, were provided by Dr. Edward Puzas, Chief of Orthopedic Research at the University of Rochester School of Medicine and Dentistry (Rochester, NY). Thawed cells were seeded on 100 mm culture dishes at 3.3×10^4 cells/dish and grown at 37°C in a 5% CO_2-humidified atmosphere with Dulbecco's modified Eagle's medium (Sigma Chemical, St. Louis, MO) supplemented with 4 mM L-glutamine, 5.6 mM glucose, 10% heat-inactivated fetal bovine serum (GIBCO, Grand Island, NY), 28 mM $NaHCO_3$, 100 IU/ml penicillin, and 100 μg/ml streptomycin sulfate. Cultures were fed by replacing the medium every 2–3 days. Cells were passaged to new culture plates every 7–10 days at an initial density one-tenth that of confluency.

The cells were harvested and used in suspension for transport studies as described in previous reports [15, 26]. Prior to harvesting, the culture medium was replaced with calcium- and magnesium-free Dulbecco's phosphate-buffered saline (Sigma/Aldrich Chemical) supplemented with 28 mM $NaHCO_3$, 0.02% EDTA, 20 mM N-2-hydroxyethylpiperazine-N′-2-ethanesulfonic acid (HEPES)-Na (pH 7.4), 100 IU/ml penicillin, and 100 μg/ml streptomycin sulfate. The cultures were incubated in this medium for 30–35 min at 37°C which causes the cells to loosen from the culture plate. Cells were aspirated off the plate and pelleted by centrifugation for 3 min at a mean centrifugal force of 380 × *g*. The cells were then resuspended in either fresh growth medium for passaging or in the appropriate medium required for a particular experimental protocol.

Membrane Potential

Membrane potentials of different polarity and magnitude were imposed experimentally in order to assess the influence of potential on the apparent K_m^{Na} for the Na^+/alanine cotransporter. Potential changes were induced by imposing diffusion potentials on suspensions of ATP-depleted cells, as described previously for intestinal epithelial cells [12, 22, 23]. Depletion of ATP was accomplished by incubating cells with 15 μg/ml valinomycin, 10 μM nigericin, and 200 μM ouabain for 20 min at 37°C in the absence of glucose. The two ionophores acting in combination are potent uncouplers of oxidative phosphorylation. Inclusion of ouabain helps ensure that the cells do not have capability for Na^+ pump activity (i.e., Na^+-gradient forming ability) due to any residual ATP remaining in the cell. LLC-PK_1 cells treated in this manner lose all capability for transport of α-methylglucoside (AMG) against a concentration gradient. They take up AMG to the same level as phlorizin-treated cells, indicating that they have lost their capacity for maintaining a Na^+-gradient and/or membrane potential. Sodium-coupled AMG transport is a 2:1 coupled cotransporter that provides a sensitive means for detection of any residual transmembrane electrochemical Na^+ gradient.

Interior Negative Membrane Potentials

An interior negative membrane potential was obtained by depleting cells of ATP in a medium containing 150 mM potassium gluconate, 10 mM N-2-hydroxyethylpiperazine-N′-2-ethanesulfonic acid neutralized to pH 7.4 with tetramethyl-ammonium hydroxide (HEPES-TMA), 2 mM $MgSO_4$, 1 mM $CaSO_4$, and 1 mg/ml bovine serum albumin. This medium facilitates depletion of intracellular [Na^+] and maintenance of high intracellular [K^+]. At the beginning of the interval for measurement of alanine influx, a 100 μl aliquot of the ATP-depleted cell suspension was added to 900 μl of incubation medium in which the slowly permeant gluconate anion was replaced by highly permeant SCN^-, and K^+ was replaced by a combination of Na^+ and piperidine$^+$. Inclusion of valinomycin (15 μM) was retained to sustain high K^+ permeability across the membrane. The resulting gradients of two highly permeant ions (inward for SCN^- and outward for K^+) established a double diffusion potential with interior negative polarity [14]. The concentration of the slowly permeant gluconate and piperidine ions can be changed without modifying the potential set by more highly permeant ions. Under these conditions, different choices for the ratio of [Na^+] to [piperidine$^+$] allow study of alanine transport at several

extracellular Na^+ concentrations without introducing a change in membrane potential.

Flux of the highly permeant tetraphenylphosphonium cation (TPP^+) was used as a means of assessing the magnitude and stability of imposed potentials at the extremes of Na^+ concentration that were studied [11, 13, 14, 23]. Linearity of TPP^+ influx during the interval in which alanine flux was measured was used as indicative of a stable membrane potential during this time period. Furthermore, stable TPP^+ influx at various $[Na^+]_o$ confirms that the diffusion potential set by the K^+ and SCN^- gradients is not compromised by the change in Na^+ gradient, at least over the range of sodium concentrations that were studied.

Interior Positive Membrane Potentials

A variation of the above approach was used to achieve interior positive membrane potentials. In this case, the cells were harvested and depleted of ATP in a medium containing 150 mM piperidine-SCN to facilitate depletion of intracellular Na^+ and K^+. In this case, alanine influx was measured immediately following addition of a 100 μl aliquot of the ATP-depleted cell suspension to 900 μl of incubation medium in which SCN^- was replaced by $gluconate^-$. $Piperidine^+$ was replaced by 30 mM K^+. Again, 15 μM valinomycin was included in the medium to maintain enhanced K^+ permeability. Different ratios of $[Na^+]$ to $[piperidine^+]$ were used to study alanine transport at various Na^+ concentrations. For these cases, the outward SCN^- gradient in conjunction with the inward K^+ gradient effectively ''clamped'' the membrane potential. TPP^+ influx was again used to show that different extracellular Na^+ concentrations can be studied under these conditions without altering the membrane potential [11, 13, 14, 17, 23].

Relative Magnitude of the Imposed Potentials

Separate experiments were conducted in which TPP^+ influx was studied for various K^+ gradients in the presence of valinomycin (no Na^+ or SCN^- present) to set K^+ equilibrium potentials. The unidirectional influx of TPP^+ for these potentials was used to define the relationship between membrane potential and infux of this permeant cation. This relationship was then used for calculating the membrane potential 'set' by the ion gradients that were imposed by the conditions described above. This technique was developed for defining the potential dependence of the Na^+-coupled sugar transporter in intestinal epithelial cells and is described in detail in earlier reports [11, 13, 14, 17, 23]. Magnitude of the interior negative and interior positive 'test' potentials as calculated by the TPP^+ influx technique was −56 and +29 mV, respectively.

Isotope Influx Measurements

The procedures employed here for measurement of alanine influx are similar to those described by Kimmich *et al.* [15, 26]. Briefly, a 100 μl aliquot of cell suspension was added to 0.9 ml of the reaction medium containing ^{14}C-L-alanine (1-2 μC/ml) and incubated at 37°C. Aliquots of the cell suspension (100 μl) were taken at 5–10 sec intervals and immediately diluted into 4 ml of ice-cold stop medium [in mM: 180 mannitol, 1 $CaCl_2$, 1 $MgCl_2$, 80 tris(hydroxymethyl)aminomethane-Cl (pH 7.4) and 1 mg/ml bovine serum albumin] followed by centrifugal separation of cells (1,000 × *g* for 25 sec). Cell pellets were resuspended in 2 ml ice-cold stop medium and centrifuged again to remove any remaining extracellular isotope from the cells. Cell pellets were dissolved in 5 ml of Ecoscint® H solubilizer (National Diagnostics, Atlanta GA), and the amount of isotope in the cells was determined by liquid scintillation spectrometry. Rates of uptake were calculated from the specific activity of isotope in the incubation medium and are given in units of nanomoles per minute per milligram of cell protein. Data for all experiments was corrected for alanine uptake observed in the absence of Na^+. At 100 μM alanine, more than 98% of the total alanine uptake by LLC-PK1 cells is Na^+-dependent [15]. The Na^+-independent uptake rate is proportional to alanine concentration over the range studies here (5 μM–2 mM), indicating that it occurs either by diffusion or via a mediated process of low affinity. All experiments were repeated at least three times. Data are presented as the mean value ± SE in each case, unless otherwise noted.

Results

The sequence of events occurring during function of any biological transport system can be broken down into four essential steps: (i) binding of extracellular substrate(s); (ii) a conformational change of the transporter/substrate complex such that substrates can be released to the opposite side of the membrane (i.e., ''translocation'' of the fully loaded transport protein); (iii) release of substrate(s) into the cytoplasm; and (iv) ''translocation'' of the substrate-free form of the transport protein so that the system is returned to its original state where new substrate molecules can gain access from the extracellular side of the membrane. For cotransport systems, if the order of substrate binding and release are known, then more detail can be added to the transport model such that binding and dissociation steps for each substrate are treated as independent events.

Alanine cotransport by LLC-PK_1 cells represents an example where considerable additional detail has been provided for the sequence of events occurring in each transport cycle [15, 26]. For that system, kinetic properties and various isotope exchange reactions have been used to show that substrate binding and release is ''ordered'' with Na^+ binding occurring prior to alanine binding at the extracellular side of the membrane, and Na^+ release occurring first at the intracellular side. For this system, the full transport cycle is best modeled using six independent transport steps occurring in the following sequence: (i) binding of extracellular sodium; (ii) binding of extracellular alanine; (iii) a conformational ''translocation'' event for the Na^+/alanine/protein complex; (iv) release of sodium at the cytoplasmic side of the membrane; (v) release of alanine into the cytoplasm; and (vi) conformational ''translocation'' of the substrate-free form of the protein to reconstitute extracellular substrate binding sites [26]. The complete transport cycle is shown schematically in Fig. 1.

For kinetic modeling, the rate of any particular step in the transport cycle is the product of a rate constant for that step and 1 or 2 additional parameters: (i) the concentration of the conformational form of the transport protein (conformer) serving as a ''reactant'' for that step and (ii) the concentration of any ''substrate'' ligands that

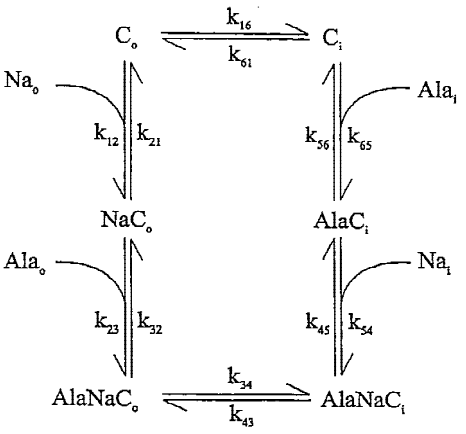

Fig. 1. Schematic diagram showing the sequence of sodium and alanine binding/dissociation events occurring during sodium-coupled alanine transport in LLC-PK_1 cells. Subscripts *i* and *o* designate intracellular and extracellular compartments, respectively for the transported substrates. For conformational states of the transport protein, subscripts show from which side of the membrane the substrates have access to their binding sites. The rate limiting step for the full transport cycle is k_{61} at high extracellular alanine concentrations [26].

interact with that conformer. Separate rate constants apply to forward and reverse events at each step. Figure 1 includes our notation for the individual rate constants for the Na^+/alanine cotransport cycle. The various states of the transporter are numbered sequentially beginning with the outward-facing conformational state of the substrate-free protein ($C_o = 1$) and proceeding counterclockwise to the corresponding inward-facing conformation of the substrate-free transporter ($C_i = 6$). Rate constant subscript numbers identify the two transporter forms that are interconverted during a particular transport step (reactant-first, product-last). Assuming that the system is at steady state, the Michaelis constant for each transported substrate can be expressed algebraically in terms of rate constants for the various steps in the transport cycle, and substrate concentrations appropriate for the experimental conditions being considered. For the model shown in Fig. 1, under zero-trans conditions (i.e., negligible intracellular Na^+ and alanine concentrations), the expression for the K_m for extracellular Na^+ (K_m^{Na}) is:

$$K_m^{Na} = \frac{S_o}{k_{12} S_s} \tag{1}$$

where

$$\begin{aligned} S_o = {} & (k_{23}[Ala]_o k_{34} k_{45} k_{56} k_{61}) + (k_{21} k_{34} k_{45} k_{56} k_{61}) \\ & + (k_{43} k_{32} k_{21} k_{16} k_{56}) + (k_{32} k_{21} k_{45} k_{56} k_{61}) \\ & + (k_{43} k_{32} k_{21} k_{56} k_{61}) + (k_{23}[Ala]_o k_{34} k_{45} k_{56} k_{16}) \\ & + (k_{21} k_{16} k_{34} k_{45} k_{56}) + (k_{32} k_{21} k_{16} k_{45} k_{56}) \end{aligned}$$

and

$$\begin{aligned} S_s = {} & (k_{34} k_{45} k_{56} k_{61}) + (k_{32} k_{45} k_{56} k_{61}) + (k_{43} k_{32} k_{56} k_{61}) \\ & + (k_{45} k_{56} k_{61} k_{23}[Ala]_o) + (k_{56} k_{61} k_{23}[Ala]_o k_{34}) \\ & + (k_{61} k_{23}[Ala]_o k_{34} k_{45}) + (k_{23}[Ala]_o k_{34} k_{45} k_{56}) \\ & + (k_{56} k_{61} k_{23}[Ala]_o k_{43}) \end{aligned}$$

Even though the K_m^{Na} can be measured readily as the Na^+ concentration required to achieve half the maximal transport rate, it is a complicated mathematical relationship that includes rate constants for all six of the primary steps in the transport cycle. Therefore, potential dependence at *any* particular step may be the basis for observed potential dependence in K_m^{Na}.

Fortunately, under certain conditions that can be achieved experimentally, the algebraic expression for the K_m^{Na} simplifies. For instance, as the extracellular alanine concentration approaches zero, those terms which include $[Ala]_o$ become negligible and the expression can be written as:

$$K_m^{Na} = \frac{\begin{array}{l} k_{21}(k_{61} k_{34} k_{45} k_{56} + k_{61} k_{32} k_{45} k_{56} + k_{61} k_{32} k_{43} k_{56} + \\ k_{16} k_{34} k_{45} k_{56} + k_{16} k_{32} k_{45} k_{56} + k_{16} k_{32} k_{43} k_{56}) \end{array}}{k_{12} k_{61} (k_{34} k_{45} k_{56} + k_{32} k_{45} k_{56} + k_{32} k_{43} k_{56})}$$

After algebraic rearrangement, the expression simplifies further to:

$$K_m^{Na} = \frac{k_{21}}{k_{12} k_{61}} (k_{61} + k_{16}) \tag{2}$$

For these conditions, K_m^{Na} is determined by rate constants relating to only two steps in the transport cycle, conformational 'translocation' of the substrate-free form of the transporter (k_{16} and k_{61}), and binding/dissociation of extracellular sodium (k_{12} and k_{21}). Potential dependence for K_m^{Na} at low alanine therefore would imply that one or both of these steps must respond to changes in the magnitude of the membrane potential.

This possibility was assessed by studying the influx of alanine as a function of Na^+ concentration for two different membrane potentials that were imposed experimentally using the methods described earlier. Figure 2 shows that influx of TPP^+ to the cells remains linear for intervals up to 36 sec in duration for an imposed diffusion potential of either polarity. Linear TPP^+ influx in turn implies that the imposed membrane potential is stable over the measurement interval. Furthermore, for either potential the TPP^+ influx remains stable when 100 mM Na^+ replaces piperidine$^+$ in the incubation medium. The rate of TPP^+ uptake is the same when Na^+ is present as in its absence. This confirms that the influence of changes in alanine transport induced by changes in extracellular Na^+ concentration can be studied under these conditions without inducing concomitant unintended changes in the magnitude of the imposed membrane potential.

A representative experiment for uptake of 2 mM L-

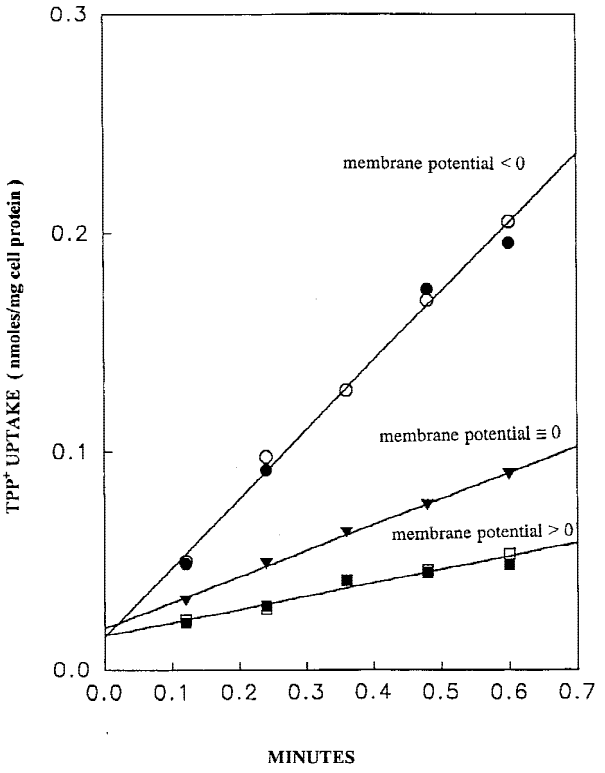

Fig. 2. Uptake of [^{14}C]TPP$^+$ at three different membrane potentials by ATP-depleted LLC-PK$_1$ cells. Circles represent uptake in the presence of an interior negative membrane potential (approximately −56 mV) established by imposing an inward gradient of SCN^- and outward K^+/gradient (in the presence of valinomycin). Squares represent uptake with an interior positive potential (approximately +29 mV) established with an inward K^+ gradient (plus valinomycin) and an outward SCN^- gradient. Triangles designate uptake in the absence of an imposed diffusion potential. This case was used for calibration of the magnitude of the imposed potentials. Open circles and squares signify uptake in the absence of sodium and closed symbols relate to uptake in the presence of 100 mM sodium.

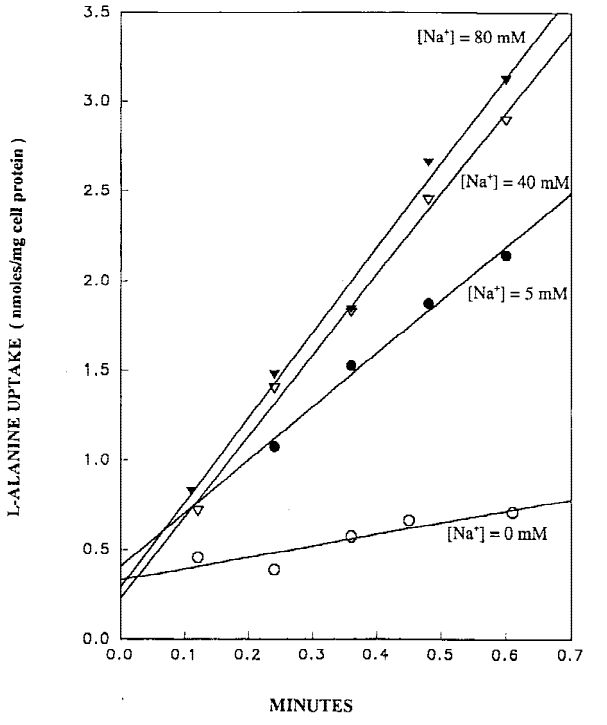

Fig. 3. Uptake of 2 mM L-alanine by ATP-depleted cells at various extracellular sodium concentrations. In each case, an inward gradient of SCN^- and an outward gradient of K^+ (in the presence of valinomycin) was imposed across the plasma membrane to establish an interior negative membrane potential. A constant membrane potential can be maintained under these conditions for changes in Na^+ concentration up to 100 mM (*see* Fig. 2). Representative data are shown for one cell population.

alanine under conditions where an interior negative membrane potential was imposed is shown in Fig. 3. For each Na^+ concentration studied, alanine uptake was linear with respect to time over the 36-sec measurement interval. Alanine uptake rates derived from similar experiments with four different cell populations were used to construct an Eadie-Hofstee plot (Fig. 4) for the relationship between alanine influx (v) and $v/[Na^+]$. The slope of each line in the plot is equal to $-K_m^{Na}$. The apparent K_m^{Na} decreases about 2-fold from 12 mM for the interior positive potential (+29 mV) to 6.8 mM for the interior negative potential (−56 mV). The V_{max} remains constant at about 4.5 nmoles/min^{-1} × mg cell protein^{-1} for the two test potentials.

Figure 5 shows the relationship between alanine influx and extracellular Na^+ concentration for the two test potentials when the alanine concentration was only 5 μM. Computer-generated least square fits of these data to the Michaelis Menten equation show that the apparent V_{max} changes by a factor of 2.7-fold for the 85 mV change in imposed test potentials (V_{max} = 0.10 ± 0.013 for the interior positive potential, and 0.27 ± 0.049 for the interior negative potential). However, at this low alanine concentration, the apparent K_m^{Na} remains constant at ~53 mM for the same 85 mV change in test potential. The slope of a Michaelis-Menten relationship is approximately equal to V_{max}/K_m at substrate concentrations below the K_m. Therefore, if the apparent K_m^{Na} remains the same for these two test potentials, one would expect the initial slope of the rate versus $[Na^+]_o$ relationship to increase by a factor of 2.7 for the data obtained at the two potentials. Indeed, the initial slope of the curves in Fig. 5 changes by a factor of 2.6 for the two cases.

Discussion

In earlier reports [15, 16], we provided evidence that at least six independent steps occur during sodium-coupled alanine transport in LLC-PK$_1$ cells as shown schematically in Fig. 1. We also showed that the rate of alanine

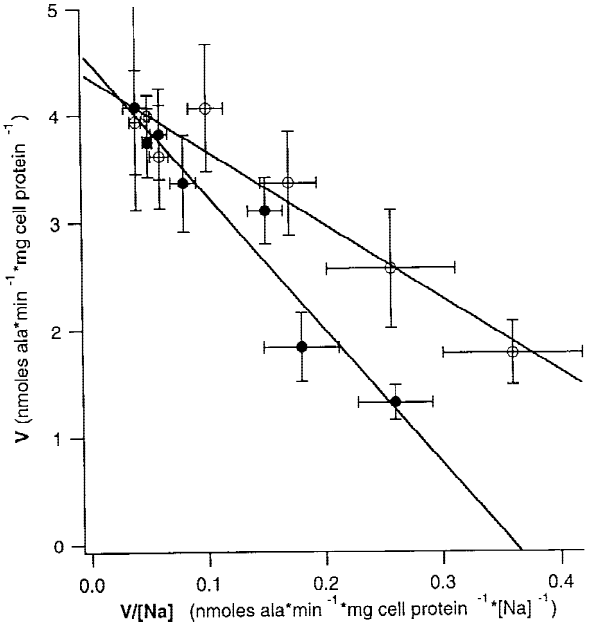

Fig. 4. Eadie-Hofstee plot of ^{14}C-alanine influx into ATP-depleted LLC-PK_1 cells at various Na^+ concentrations when the extracellular alanine is held constant at 2 mM. Open circles indicate data taken in the presence of an interior negative membrane potential, and solid circles are for an interior positive potential. The lines are computer generated least squares fit of the data to the general equation for a straight line. Data were pooled from four separate cell populations and normalized to the maximal velocity achieved for the specific cell population from which it was collected before pooling. Error bars indicate the standard error and are shown unless they are smaller than the symbol used. The negative slope of each line is the apparent K_m^{Na} for that potential: 6.9 mM for the interior negative potential and 15.6 mM when the potential is interior positive.

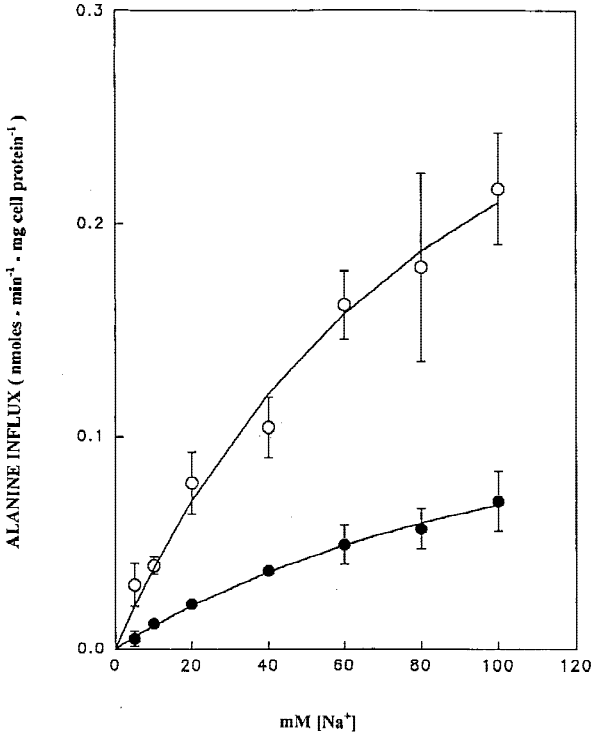

Fig. 5. The rat of L-alanine uptake by ATP-depleted LLC-PK_1 cells as a function of sodium concentration when the extracellular alanine concentration is held constant at 5 μM for two different membrane potentials. Open circles indicate uptake in the presence of an interior negative membrane potential, and closed circles in the presence of an interior positive potential. Data were pooled from four separate cell populations without normalization. The curves show the least squares fit of the pooled data to the Michaelis-Menten equation. Error bars indicate the standard error and are shown unless they are smaller than the symbol used. Computer generated values for the apparent K_m^{Na} and apparent V_{max} were 50 mM and 0.27 nmol × min^{-1} × mg cell $protein^{-1}$ for the interior negative potential, and 56 mM and 0.1 nmol × $min.^{-1}$ × mg cell $protein^{-1}$ for the interior positive potential.

transport in these cells responds to changes in the magnitude of the membrane potential [15] which implies that one or more steps in the transport cycle must be potential dependent. Identifying the site(s) of potential dependence may provide important insight to the regulation of molecular events in the cotransport cycle, and it is that aim which forms the basis of this report.

Because it is difficult to define conditions that allow measurement of the magnitude or potential dependence of rate constants associated with a specific transport step, it is usually necessary to identify situations in which insight can be derived from measureable kinetic parameters such as the V_{max} and K_m. However, as mentioned earlier, for cotransport systems these parameters are complex algebraic expressions consisting of multiple terms that include rate constants for every step in the full transport cycle. Equation 1 provides an example for the Na^+/alanine cotransporter. Even when intracellular substrates are absent, the expression for the K_m^{Na} for this 1:1 coupled system has 8 numerator and 8 denominator terms, in which each term is the product of 5 different rate constants. Fortunately, at low alanine concentrations the expression simplifies to the form given by equation 2 with rate constants for only two sites in the cycle. Under these conditions, the K_m^{Na} offers an ideal opportunity for assessing whether either of these loci exhibits potential dependence.

Because the K_m for any transported solute is the concentration required to achieve half maximal transport velocity, K_m is sometimes incorrectly interpreted as a measure of the ''affinity'' of the transport protein for the solute. If K_m^{Na} is equated with Na^+ affinity, it would be concluded that sodium binding and dissociation are potential dependent given the fact that the apparent K_m^{Na} is markedly dependent on the magnitude of the membrane potential when the alanine concentration is 2 mM (Fig. 4). Indeed, 6 of the 8 numerator terms in the full expression for K_m^{Na} (Eq. 1) include the rate constant for Na^+ dissociation (k_{21}), which might suggest that potential dependence for this constant will be reflected in a potential-

dependent apparent K_m for Na^+. True chemical affinity of the protein for extracellular Na^+ is the ratio of rate constants governing binding and release of Na^+ (k_{12}/k_{21}).

However, when the alanine concentration is lowered to 5 μM the same 85 mV change in potential induces no change in the apparent K_m^{Na} (Fig. 5) despite the fact that under these conditions the expression for K_m^{Na} simplifies to one in which the rate constants for binding/release of extracellular sodium (i.e., constants associated with the true affinity of the transporter for Na^+) have even greater weighting. The data obtained at low [alanine] are not compatible with a potential-dependent shift in Na^+ affinity, and therefore are inconsistent with a Na^+-well conceptual model. The data *in toto* also emphasizes the faulty logic in equating Michaelis constants with affinity of the transport protein for substrate ligands.

It is important to recognize that the algebraic simplification in the expression for K_m^{Na} requires a very low concentration of extracellular alanine relative to the K_m for alanine. A test alanine concentration of 5 μM was chosen for these studies because it is 50-fold lower than the apparent K_m^{Na} of 240 μM, reported earlier for these cells at 135 mM $[Na^+]_o$ [15, 26]. If this concentration is truly low enough to satisfy the assumption that $[Ala]_o \rightarrow 0$, then the K_m^{Na} should be independent of [alanine] at other concentrations near this value. For this reason, we repeated the experiment with a 2-fold higher extracellular alanine concentration (10 μM) in the presence of an interior negative membrane potential. Under these conditions, the apparent K_m^{Na} was 52 mM (*data not shown*), or the same as that determined with 5 μM extracellular alanine.

Previously, we reported evidence indicating that 'translocation' of the substrate-free protein is rate limiting for the full transport cycle at concentrations of alanine usually employed in kinetic studies [26]. Here we have shown that lowering extracellular alanine to 5–10 μM can be used to create a new rate limiting step. Of course, a low alanine concentration does not change the magnitude of the rate constant k_{23}, but at a sufficiently low level the rate of the transport cycle becomes dependent on the $k_{23}[Ala]_o$ product. The fact that rate limitation due to $[Ala]_o$ occurs for concentrations on the order of 5–10 μM implies that in this range the magnitude of the $k_{23}[Ala]_o$ product must be less than the usually limiting value of k_{61}.

It is possible to calculate the ratio of k_{61} to $k_{23}[Ala]_o$ that is necessary to satisfy the requirements for the algebraic simplification. To do so, we compared the apparent K_m^{Na} calculated using the simplified expression (Eq. 2) with computed values using the full expression (Eq. 1). The simplification is valid with 95% accuracy when k_{61} is at least 25 times greater than k_{23}[Ala] regardless of the magnitude of the other rate constants, provided that the other constants are at least 10-fold greater than k_{61}.

Lack of potential dependence for K_m^{Na} at very low extracellular alanine concentrations suggests one of two conclusions: (i) neither step (translocation of the substrate-free form of the transporter nor binding/dissociation of extracellular sodium) is potential dependent or (ii) both steps are potential dependent but in a manner in which changes in membrane potential affect flux in an opposing sense such that the two changes nullify one another. The latter explanation would require that at least one of the two sites allows influence by the membrane potential which opposes transport activity, in contrast to the well known potential-induced transport enhancement for this and many other Na^+-coupled systems. Opposing effects which just cancel one another also seem unlikely for several different cell populations subjected to the large change in potential that was tested. Therefore, even though the K_m^{Na} is potential dependent at higher extracellular alanine concentrations, it is unlikely that this is due to potential dependent binding/dissociation of sodium.

This conclusion differs from that drawn from our studies of Na^+-coupled sugar transport in LLC-PK_1 cells. In that case, the collective data are consistent with a Na^+-well concept [3, 4, 12]. The two conclusions suggest that there is no general paradigm that can be used to explain the basis of potential dependence for all Na^+-coupled transport systems. The lack of potential dependence in the apparent K_m^{Na} when extracellular alanine binding is rate limiting also suggests that 'translocation' of the free carrier does not respond to the membrane potential despite the fact that isotope exchange experiments indicate that this step is rate limiting for the full transport cycle at high concentrations of extracellular alanine. A wholly adequate explanation for the site of potential dependence for the Na^+/alanine cotransporter remains to be identified.

This work was supported by a grant from the USPHS (No. DK-15365-24).

References

1. Aidley, D.J. 1989. The Physiology of Excitable Cells. 3rd. ed. Cambridge University Press, Cambridge
2. Aronson, P. 1984. Electrochemical driving forces for secondary active transport: Energetics and kinetics of Na^+-H^+ exchange and Na^+-glucose cotransport. *In:* Electrogenic Transport: Fundamental Principles and Physiological Implications. M.P. Blaustein and M. Lieberman editors. pp. 49–70. Raven, New York
3. Bennett, E., Kimmich, G.A. 1992. Na^+ binding to the Na^+-glucose cotransporter is potential dependent. *Am. J. Physiol.* **262:**C510–C516
4. Bennett, E., Kimmich, G.A. 1996. The molecular mechanism and potential dependence of the Na^+/glucose cotransporter. *Biophys. J.* **70:**1676–1688
5. Chen, X.-Z., Coady, M.J., Lapointe, J.-Y. 1996. Fast voltage clamp

discloses a new component of presteady-state currents from the Na^+-glucose cotransporter. *Biophys. J.* **71:**2544–2552

6. Chen, X.-Z., Coady, M.J., Jackson, F., Berteloot, A., Lapointe, J.-Y. 1995. Thermodynamic determination of the Na^+: glucose coupling ratio for the human SGLT1 cotransporter. *Biophys. J.* **69:**2405–2414
7. Fitz, J.G., Lidofsky, S.D., Scharschmidt, B.F. 1993. Regulation of hepatic Na^+-HCO_3-cotransport and pH by membrane potential difference. *Am. J. Physiol.* **265:**G1–G8
8. Hille, B. 1992. Ionic Channels of Excitable Membranes. 2nd. edition. Sinauer, Sutherland, MA
9. Hoyer, J., Gögelein, H. 1991. Sodium-alanine cotransport in renal proximal tubule cells investigated by whole-cell current recording. *J. Gen. Physiol.* **97:**1073–1094
10. Kessler, M., Semenza, G. 1983. The small intestine Na^+, D-glucose cotransporter: An asymmetric gated channel (or pore) responsive to changes in membrane potential. *J. Membrane Biol.* **76:**27–56
11. Kimmich, G.A. 1986. Non-invasive measurement of membrane potentials: Na^+-dependent sugar transport as a quantitative sensor. *In:* Ion Gradient-Coupled Transport INSERM Symposium No. 26. F. Alvarado and C.H. van Os, editors. Elsevier Science Publishers B.V.
12. Kimmich, G.A. 1990. Membrane potentials and the mechanism of intestinal Na^+-dependent sugar transport. *J. Membrane Biol.*, **114:**1–27
13. Kimmich, G.A., Randles, J., Restrepo, D., Montrose, M. 1985. The potential dependence of the intestinal Na^+-dependent sugar transporter. *Ann. NY Acad. Sci.* **456:**63–76
14. Kimmich, G.A., Randles, J., Restrepo, D., Montrose, M. 1985. A new method for determination of relative ion permeabilities in isolated cells. *Am. J. Physiol.* **248:**C399–C405
15. Kimmich, G.A., Randles, J., Wilson, J.J. 1994. Na^+-coupled alanine transport in LLC-PK_1 cells. *Am. J. Physiol.* **267:**C1119–C1129
16. Läuger, P., Jauch, P. 1986. Microscopic description of voltage effects on ion-driven cotransport systems. *J. Membrane Biol.* **91:**275–384
17. Lu, C.C., Kabakov, A., Markin, V.S., Mager, S., Frazier, G.A., Hilgemann, D.W. 1995. Membrane transport mechanisms probed by capacitance measurements with megahertz voltage clamp. *Proc. Natl. Acad. Sci.* **92:**11220–11224
18. Maloney, P.C. 1982. Energy coupling to ATP synthesis by the proton-translocating ATPase. *J. Membrane Biol.* **67:**1–12
19. Mackenzie, B., Loo, D.D.F., Panayotova-Heiermann, M., Wright, E.M. 1996. Biophysical characteristics of the pig kidney Na^+/glucose cotransporter SGLT2 reveal a common mechanism for SGLT1 and SGLT2. *J. Biol. Chem.* **271:**3678–3683
20. Mitchell, P. 1969. Chemiosmotic coupling and energy transduction. *Theor. Exp. Biophys.* **2:**159–216
21. Parent, L., Supplisson, S., Loo, D.D.F., Wright, E.M. 1992. Electrogenic properties of the cloned Na^+/glucose cotransporter. I: Voltage-clamp studies. *J. Membrane Biol.* **125:**49–62
22. Restrepo, D., Kimmich, G.A. 1985. The mechanistic nature of the membrane potential dependence of sodium-sugar cotransport in small intestine. *J. Membrane Biol.* **87:**159–172
23. Restrepo, D., Kimmich, G.A. 1986. Phlorizin binding to isolated enterocytes: Membrane potential and sodium dependence. *J. Membrane Biol.* **89:**269–280
24. Schwartz, E.A., Tachibana, M. 1990. Electrophysiology of glutamate and sodium cotransport in a glial cell of the salamander retina. *J. Physiol.* **426:**43–80
25. Tannenbaum, C., Toggenburger, G., Kessler, M., Rothstein, A., Semenza, G. 1977. High-affinity phlorizin binding to brush border membranes from small intestine: identity with (a part of) the glucose transport system, dependence on Na^+-gradient, partial purification. *J. Supramol. Struct.* **6:**519–533
26. Wilson, J.J., Randles, J., Kimmich, G.A. 1996. A model for the kinetic mechanism of sodium-coupled L-alanine transport in LLC-PK_1 cells. *Am. J. Physiol.* **270:**C49–C56